Comparison of the Beta-Alpha Angular Correlations in the Li^8 and B^8 Beta Decays, and the Conserved Vector Current Theory*

M. E. Nordberg, Jr., F. B. Morinigo, and C. A. Barnes
California Institute of Technology, Pasadena, California

(Received August 21, 1961)

This paper describes a comparison of the beta-alpha angular correlations of the beta decays of Li^8 and B^8 to the 2.90-Mev alpha-unstable level of Be^8. The data were fitted to an angular correlation in the laboratory system of the form $W(\theta_{\beta\alpha})=1+A\cos\theta_{\beta\alpha}+B\cos^2\theta_{\beta\alpha}$, where A and B were independently determined for the Li^8 and B^8 beta decays from measurements at $\theta_{\beta\alpha}=0°$, 90°, and 180°. The coefficients A are due to the recoil of Be^{8*} and have the same sign for both beta decays. The coefficients B arise from the interference of forbidden vector matrix elements with the allowed axial vector matrix element and have different signs in the two decays. The correlation for the Li^8 decay was measured with average total beta energies, $W_\beta\simeq 5$, 8, and 11 Mev. Both A and B were found to be approximately linear in W_β. The correlation for the B^8 decay was measured only with average $W_\beta\simeq 11$ Mev. From the data with $W_\beta\simeq 11$ Mev, the difference of the coefficients, $B(Li^8)-B(B^8)$, equals $(0.0070\pm 0.0012)W_\beta$. This result is compared with theoretical predictions based on the older Fermi and the newer conserved vector current theories of beta decay. The experiment agrees with the prediction of the latter theory.

I. INTRODUCTION

A. Conserved Vector Current Theory

ON theoretical grounds, it has been proposed that the weak interactions have a universal form, vector-axial vector $(V-A)$, and also a universal strength.[1–3] In nuclear beta decay, the proposed $V-A$ form predicts a degree of parity nonconservation in good agreement with experiment.[4] The hypothesis of universal strength has found support in that the coupling constant in the muon decay, G_μ, and the vector coupling constant in the O^{14} decay, G_V, have been shown experimentally to be nearly equal.[5,6] The remaining 1.8% difference may be due to inadequate calculation of small theoretical corrections to the two decay rates, or to a weak charge-dependent nuclear force.[7] This near equality of G_V and G_μ is, at first sight, surprising, since one might expect a large renormalization of G_V due to the coupling of nucleons to pions, whereas the muon apparently has no strong couplings.

As an explanation of the apparent absence of a renormalization of G_V, Feynman and Gell-Mann[1] proposed that the weak interactions can be represented by the self interaction of a weak, vector plus axial vector current, and that the vector part of the weak current is conserved by including pion contributions as well as nucleon contributions, in the same way that the electromagnetic current is conserved by including pion currents as well as nucleon currents.

Gell-Mann[8] has suggested, as a test of the conserved vector current (C.V.C.) hypothesis, a comparison of the deviations from a simple allowed shape of the beta spectra of B^{12} and N^{12}. In these predominantly axial vector transitions, small interference terms should be produced by second forbidden vector transitions as well as by other forbidden transitions. By extending the analogy between the electromagnetic current and the weak vector current, Gell-Mann showed that the forbidden vector beta transitions should be enhanced by contributions from the pion weak current in the same way that the corresponding $M1$ gamma transition from the analogue $T=1$ state in C^{12} is enhanced by the anomalous magnetic moments of the nucleons (the so-called "weak-magnetism" effect). The known strength of this $M1$ gamma transition makes possible a quantitative prediction of the enhancement of the vector beta transition, since the same nuclear matrix elements occur in the vector beta decay as in the $M1$ gamma transition. A recent study, in this laboratory, of the B^{12} and N^{12} spectral shapes is in agreement with the predictions of the conserved vector current hypothesis.[9]

B. Li^8 and B^8 Beta-Alpha Angular Correlations

Bernstein and Lewis,[10] and Morita[11] have shown that second forbidden vector interference terms should also lead to deviations from isotropy in the beta-alpha angular correlations of the Li^8 and B^8 beta decays. These mirror nuclei decay primarily by an allowed Gamow-Teller transition to the 2.90-Mev level of Be^8 which promptly decays into two alpha particles. The mass-8 triplet is illustrated in Fig. 1, in which the dashed line represents the $M1$ gamma transition to the 2.90-Mev level of Be^8, from the $J=2^+$, $T=1$ level,

* Supported in part by the Joint Program of the Office of Naval Research and the U. S. Atomic Energy Commission.

[1] R. P. Feynman and M. Gell-Mann, Phys. Rev. **109**, 193 (1958).
[2] E. C. G. Sudarshan and R. E. Marshak, Phys. Rev. **109**, 1860 (1958).
[3] J. J. Sakurai, Nuovo cimento **7**, 649 (1958).
[4] A summary of recent experimental results and theoretical interpretations is given by E. J. Konopinski, Ann. Rev. Nuclear Sci. **9**, 99 (1959).
[5] R. K. Bardin, C. A. Barnes, W. A. Fowler, and P. A. Seeger, Phys. Rev. Letters **5**, 323 (1960).
[6] J. W. Butler and R. O. Bondelid, Phys. Rev. **121**, 1770 (1961).
[7] R. J. Blin-Stoyle and J. Le Tourneux, Phys. Rev. **123**, 627 (1961).
[8] M. Gell-Mann, Phys. Rev. **111**, 362 (1958).
[9] T. Mayer-Kuckuk and F. C. Michel, Phys. Rev. Letters **7**, 167 (1961).
[10] J. Bernstein and R. R. Lewis, Phys. Rev. **112**, 232 (1958).
[11] M. Morita, Phys. Rev. **113**, 1584 (1959).

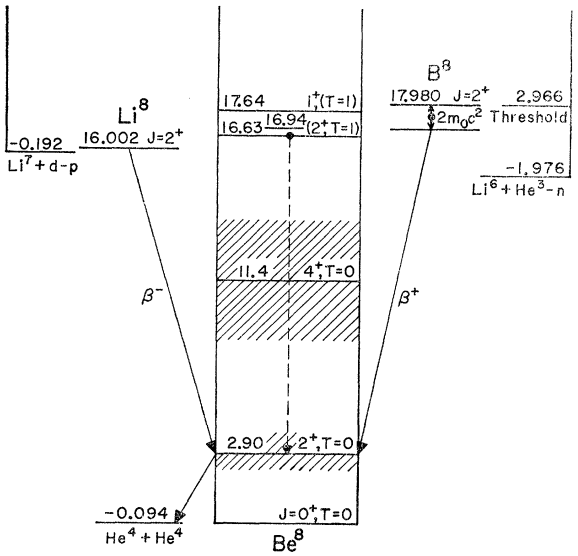

FIG. 1. Energy level diagram and the mass-8 triad. The Li^8 electron decay and the B^8 positron decay are followed by the α-particle breakup of the 2.90-Mev Be^{8*} level.

analogous to the Li^8 and B^8 ground states.[12] The angular correlation in the rest system of Be^{8*}, due to the $M1$ type vector-axial vector interference, was shown to be[10,11]

$$W(\theta_{\beta\alpha}) \simeq 1 + aW_\beta \cos^2\theta_{\beta\alpha}, \tag{1}$$

where $\theta_{\beta\alpha}$ is the angle between the electron and one alpha particle, and W_β is the total energy of the electron (in the approximation $W_\beta \simeq p_\beta c$).

The quantity, a, defined by Gell-Mann,[8] is

$$a = \frac{\mathfrak{y}}{\sqrt{2}Mc^2\lambda\mathfrak{M}}, \tag{2}$$

where M is the nucleon mass, $\lambda = -G_A/G_V \simeq 1.2$, $\mathfrak{M}$ is the allowed axial vector matrix element, and $\mathfrak{y}$ is the transition magnetic moment (in nuclear magnetons). $\mathfrak{y}$ can be calculated from the $M1$ gamma-transition rate,

$$\Gamma_\gamma(M1) = \frac{\mathfrak{y}^2\omega^3}{3(137)M^2c^4}, \tag{3}$$

where ω is the energy of the gamma ray. The allowed Gamow-Teller matrix element, $\mathfrak{M}$ is obtained from a comparison of the Li^8 or B^8 ft value (5×10^5) with that of the pure Fermi beta transition in O^{14}, for which the matrix element equals $\sqrt{2}$. Thus,

$$a = -\frac{1}{\omega}\left[\frac{3}{4}\left(\frac{137\Gamma_\gamma}{\omega}\right)\frac{ft}{(ft)_{O^{14}}}\right]^{\frac{1}{2}}. \tag{4}$$

The sign of a is not determined in this analysis. Since the sign of a changes between the Li^8 and B^8 decays, a comparison of the two correlations measures twice the asymmetry of one decay alone. Indeed, it is imperative to make a comparison of the two correlations because there are many terms which can lead to small asymmetries having the same sign in both decays. Defining δ as the difference of the $\cos^2\theta_{\beta\alpha}$ terms in the Li^8 and B^8 angular correlations, inserting the ft-values quoted above, and taking $\omega = 13.7$ Mev, we have

$$\delta = |2aW_\beta| \simeq 0.005[\Gamma_\gamma(M1)]^{\frac{1}{2}}W_\beta, \tag{5}$$

where $\Gamma_\gamma(M1)$ is measured in ev and W_β in Mev.

C. Theoretical Estimates of $\Gamma_\gamma(M1)$

The $J=2^+$, $T=1$ level of Be^8 has not been identified with certainty but it is probably either the 16.94- or the 16.63-Mev level of Fig. 1[12,13]; from the $Li^7(d,n)Be^{8*}$ $L=1$ stripping pattern it is likely the latter.[14] Since the gamma-transition rate to the 2.90-Mev, $J=2^+$, $T=0$ level has not been experimentally determined, Bernstein and Lewis[10] assumed the average value in light nuclei given by Wilkinson[15]: $\Gamma_\gamma(M1) = 0.15\Gamma_W$, where Γ_W is the Weisskopf unit. With this estimate, $\Gamma_\gamma(M1) = 8.2$ ev and δ is predicted to be $(0.015)W_\beta$.

A preliminary study[16] of the angular correlations yielded $\delta = (0.002\pm0.004)W_\beta$, where the quoted error is of statistical origin only, a result in disagreement with this prediction. No conclusion could be reached concerning the validity of the conserved vector current theory, however, in view of the large uncertainty in the estimate of $\Gamma_\gamma(M1)$.

In order to provide more reliable estimates of $\Gamma_\gamma(M1)$, Weidenmüller[17] and Kurath[18] have fitted the pertinent energy levels of the mass-8 system with the intermediate coupling model. Weidenmüller's calculation indicated that 1 ev $\leq\Gamma_\gamma(M1)\leq$ 4 ev, including estimates of the spin-orbit-coupling term in the Hamiltonian. The value of $\Gamma_\gamma(E2)$, which could also lead to anisotropies that would not cancel in taking the difference δ, was estimated to be negligible. These calculations also enabled Weidenmüller to determine the deviation from isotropy which could be expected from the older Fermi theory where no pion corrections are made. If $\mathbf{l}$ is the orbital angular momentum operator and $\boldsymbol{\sigma}$ the spin operator the Fermi theory predicts an asymmetry proportional to $\langle|\mathbf{l}+\boldsymbol{\sigma}|\rangle$ and the conserved vector current theory predicts an effect proportional to $\langle|\mathbf{l}+4.7\boldsymbol{\sigma}|\rangle$. Quanti-

[12] F. Ajzenberg-Selove and T. Lauritsen, Nuclear Phys. **11**, 1 (1959).

[13] J. R. Erskine and C. P. Browne, Bull. Am. Phys. Soc. **5**, 230 (1960).

[14] F. S. Dietrich and L. Cranberg, Bull. Am. Phys. Soc. **5**, 493 (1960).

[15] D. H. Wilkinson, *Nuclear Spectroscopy B*, edited by F. Ajzenberg-Selove, (Academic Press, Inc., New York, 1960), 1st ed., p. 852.

[16] M. E. Nordberg, B. Povh, and C. A. Barnes, Phys. Rev. Letters **4**, 23 (1960).

[17] H. A. Weidenmüller, Phys. Rev. Letters **4**, 299 (1960).

[18] D. Kurath, Phys. Rev. Letters **4**, 180 (1960).

tatively, Weidenmüller predicts

$$\text{Fermi theory } (0.001)W_\beta<\delta<(0.004)W_\beta,$$
$$\text{C.V.C. theory } (0.005)W_\beta<\delta<(0.009)W_\beta.$$

The calculation predicts that a is positive for Li^8. Kurath finds for the conserved-current theory a value of δ near the upper limit of Weidenmüller's calculation. Thus, on the basis of the intermediate coupling model calculations the asymmetry predicted by the conserved vector-current theory is about a factor of two smaller than the original estimate of Bernstein and Lewis, and the new conserved vector-current theory and the older Fermi theory predict similar asymmetries differing in magnitude by about a factor of two. Both of these facts make the experimental differentiation between the theories more difficult.

Morita has made rough approximations to the various matrix elements in order to estimate the effect on the Li^8 and B^8 beta-alpha angular correlations.[11] He estimates a value of δ about $(0.005)W_\beta$ for the conserved vector current theory and $(0.002)W_\beta$ for the older theory with no pion corrections.

The result of the present experiment is

$$\delta=(0.0070\pm0.0012)W_\beta$$

(where the quoted error is the statistical error combined with estimates of systematic errors), which is in agreement with the prediction of the conserved vector current theory.[19]

D. Angular Correlation in the Laboratory System

In the laboratory system the largest terms in the beta-alpha angular correlation can be written in the general form,

$$W(\theta_{\beta\alpha})=1+A\cos\theta_{\beta\alpha}+B\cos^2\theta_{\beta\alpha}. \quad (6)$$

The appearance of the $\cos\theta_{\beta\alpha}$ term is a kinematic effect; this term arises in transforming the correlation from the Be^{8*} rest system to the laboratory system, and to first order is $-W_\beta/p_\alpha c$,[20] where W_β and p_α are the electron total energy and the alpha-particle momentum, respectively. The same kinematic effect causes the shift with angle of the laboratory energy of the coincident alpha spectra, which is evident in Figs. 7 and 8. The transformation has been carried out to second order in terms containing W_β, including only kinematic effects and the interference of the vector $M1$-type matrix element characterized by a. The neutrino momentum does not contribute to the first-order terms, and second-order terms involving the neutrino momentum were neglected. This procedure, which is outlined in Appendix A, gives

$$W(\theta_{\beta\alpha})=1+\left[\frac{W_\beta}{c}\langle 1/p_\alpha\rangle+\frac{3aW_\beta^2}{2c}\langle 1/p_\alpha\rangle\right]\cos\theta_{\beta\alpha}+\left[aW_\beta+\frac{5W_\beta^2}{8c^2}\langle 1/p_\alpha\rangle^2\right]\cos^2\theta_{\beta\alpha}. \quad (7)$$

In this expression, $\langle 1/p_\alpha\rangle$ means the average value of $1/p_\alpha$ for the laboratory α spectrum in coincidence with electrons at 90°. Since the second term in the coefficient of $\cos^2\theta_{\beta\alpha}$, and the neglected axial vector-axial vector interference terms, are approximately the same for both the Li^8 and the B^8 decay, they drop out in taking the difference, $\delta=B(Li^8)-B(B^8)=2aW_\beta$.

In order to determine the coefficients, A and B, for both beta decays, it is necessary to measure the number of coincidences at least at three values of angle, $\theta_{\beta\alpha}$; the angles 0°, 90°, and 180° were chosen in this experiment. After integrating over the solid angles of the beta and alpha counters, which were defined by circular apertures subtending half-angles of 19°40′ and 9°, respectively, the coefficients A and B are given by

$$A=\frac{n(0°)-n(180°)}{1.930n(90°)}, \quad (8)$$

$$B=\frac{n(0°)+n(180°)+2n(90°)}{1.864n(90°)-0.034[n(0°)-n(180°)]}, \quad (9)$$

where $n(\theta)$ is the normalized coincidence rate at the angle θ. In some of our earlier work coincidences were measured only at 90° and 180°. From these measurements the coefficient B was determined from the expression,

$$B=\frac{n(180°)-[1-0.965A]n(90°)}{0.932n(90°)-0.034n(180°)}, \quad (10)$$

where the value of A was determined from the 3-angle measurements.

II. APPARATUS

A. Target Chamber and Counting Arrangement

The angular distributions were measured by counting coincidences between alpha-particles detected in a gold-silicon surface-barrier detector and electrons or positrons detected in a plastic scintillator which could be rotated about the target to positions of 0°, 90°, or 180° relative to the alpha-detector (to positions of 90° or 180° in an earlier target chamber). The Li^8 and B^8 target nuclei were produced in the nuclear reactions,[12]

$Li^7(d,p)Li^8$ $Q=-0.192$ Mev, threshold $=0.247$ Mev,

$Li^6(He^3,n)B^8$ $Q=-1.976$ Mev, threshold $=2.966$ Mev.

The beams of deuterons or He^3 ions were accelerated by a Van de Graaff electrostatic generator and analyzed

[19] M. E. Nordberg, F. B. Morinigo, and C. A. Barnes, Phys. Rev. Letters 5, 321 (1960).

[20] We are indebted to B. Stech and J. Eichler for pointing out an error in the A coefficient used in the analysis of our preliminary experiment.

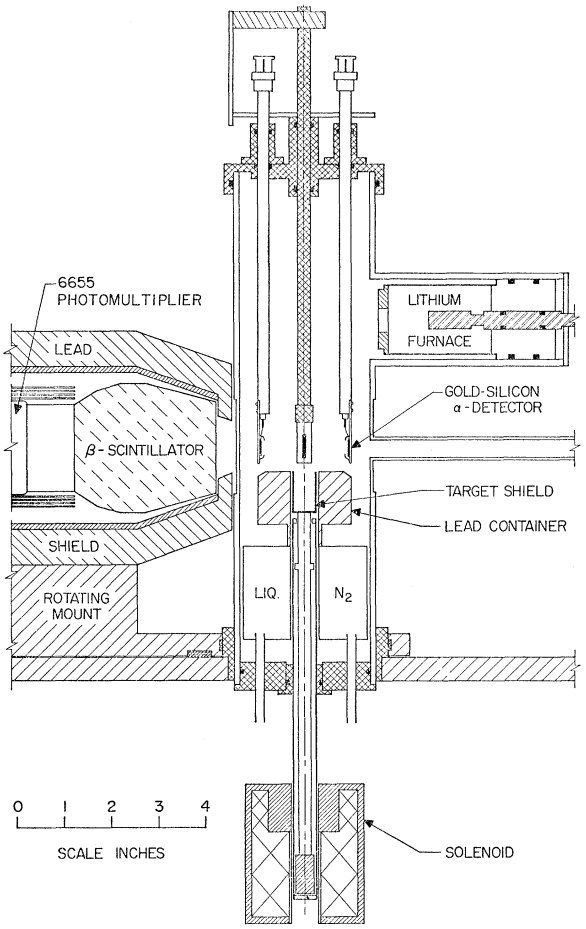

FIG. 2. Vertical section of the target chamber and detectors. The lithium target was evaporated in a narrow strip onto the target backing while it was raised to the lithium furnace. The target shield, shown in the counting position, was raised when the beam irradiated the target.

in a 90° double-focusing magnet at 0.75 Mev and 3.2 Mev, respectively.

The target chamber and the general counting arrangement are shown in Figs. 2 and 3. The chamber consisted of a 3-in diam by $\frac{1}{8}$-in.-wall Lucite tube. Mounted in it were the alpha detectors, a liquid nitrogen cold trap, a 5-mil aluminum target backing, a movable shield to surround the target, and a lead container for this shield. In Fig. 3, the alpha detector at the bottom is the coincidence counter, the one to the right is used as a monitor, and the remaining two are included to maintain symmetry. In addition, the chamber wall was turned to a uniform thickness to preserve symmetry.

The target materials were natural lithium (92.6% Li^7 and 7.4% Li^6) for the Li^8 decay and enriched Li^6 (99.7% Li^6) for the B^8 decay. The lithium was evaporated inside the vacuum chamber, as a 2-mm wide vertical strip on a 5-mil aluminum backing. The angle of incidence of the beam was 75° so that the projection of the lithium strip on the plane perpendicular to the direction of the beam ($\sim\frac{1}{2}$ mm) was narrower than the beam width ($\sim$1 mm). Therefore, the position of the radioactive source was defined by the lithium strip rather than the beam, and thus the possibility of changes in the counter solid angles arising from lateral motion of the beam was minimized. The primary reason for the 75° angle of incidence was to reduce the recoil of the Li^8 or B^8 in a direction perpendicular to the surface of the aluminum backing, and thereby, to reduce the energy loss of the alpha particles in coming back out. This recoil was unavoidably different in the two cases and was greater in the case of B^8 because of the higher mass and energy of the incident beam (3.2-Mev He^3 vs 0.75-Mev deuterons). In order to ensure that no systematic effect in the angular correlation would be produced by the small remaining differences in the shape of the alpha spectra, the coincident alpha spectra were recorded on a 100-channel analyzer and extrapolation was made to zero pulse height.

Coincidences were recorded in a delayed period after the beam was turned off. A one-second cycle was chosen in order that mechanical choppers could be used and in order to be compatible with the half lives of Li^8 and B^8 of 0.848 sec and 0.77 sec, respectively. During each 1-sec cycle the beam was on the target for 0.4 sec and

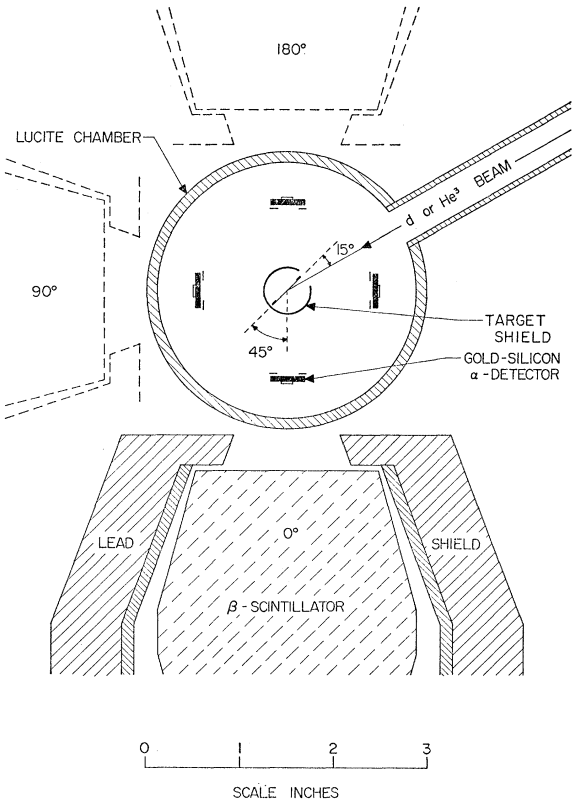

FIG. 3. Horizontal section of the target chamber and detectors. Coincidences between alpha particles in the lower gold-silicon alpha detector and electrons in the beta scintillator were recorded as a function of their relative angle.

off for 0.6 sec; the scalers and 100-channel analyzer were off 0.6 sec and on 0.4 sec, and the shield surrounded the target 0.5 sec and dropped out of the way into its lead container 0.5 sec. The purpose of this shield was twofold. (1) It allowed the beam to enter through a small hole but caught any radioactive nuclei that recoiled out of the target. Any Li^8 or B^8 atoms reaching the target chamber wall would have produced an asymmetrical source of electrons or positrons. During the counting period of the cycle the target shield dropped into its lead container which completely absorbed electrons from the shield. (2) The second purpose of the shield was to prevent sputtered target material from reaching the gold-silicon alpha detectors. This was especially important in the B^8 case where a more intense and higher energy beam was incident on the target.

B. Detectors and Electronic Circuitry

For the alpha detector, a gold-silicon surface-barrier detector was chosen because of its fast rise time, low sensitivity to beta rays, linear response to low-energy alpha particles, and simplicity of construction.[21] Operated at a bias of -10 v, the detector response was linear in alpha-particle energy to about 8 Mev, which is well beyond the 1.5-Mev peak of the observed alpha-particle group. The detector was constructed from a $\frac{1}{32}$-in. thick by $\frac{5}{16}$-in. square wafer of etched 1500 ohm-cm silicon on which a thin gold layer was evaporated. A $\frac{1}{4}$-in. aperture was placed in front of the detector and it was positioned about $\frac{7}{8}$-in. from the target. New detectors were constructed occasionally throughout the experiment because of deterioration with use in the vacuum system.

The beta-detector was a shaped plastic scintillator fastened to an RCA type 6655 photomultiplier. The photomultiplier was shielded from stray magnetic fields and the scintillator was encased in a lead housing to reduce background gamma radiation. The scintillator had a maximum diameter of $2\frac{3}{4}$-in. tapering to 2-in., whereas the aperture of the lead shield was only $1\frac{3}{8}$ in. The smaller aperture reduced the probability of high-energy beta rays scattering out of the scintillator. The pulse height resolution was about 10% for high-energy electrons.

The electronic circuitry was a standard "slow-fast" coincidence arrangement, as shown in Fig. 4. Charge integrating pre-amplifiers were used with both the alpha detector and the beta photomultiplier. In the fast circuit these were followed by Hewlett-Packard delay-line amplifiers, clippers, limiters, and a coincidence mixer of either a 6BN6-type or a tunnel diode type. An 80-nsec resolving time was used. The slow

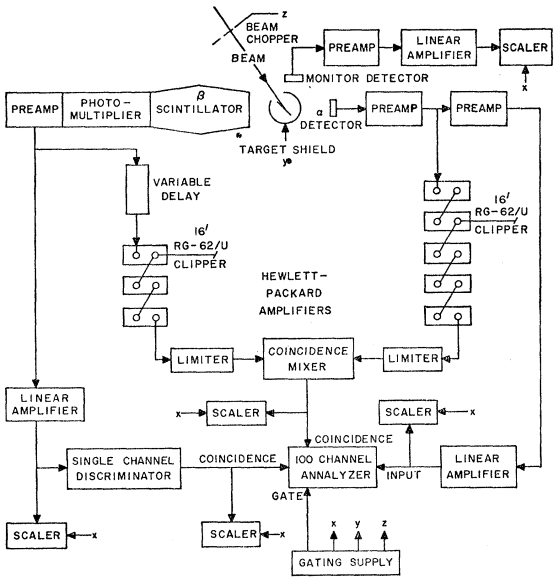

FIG. 4. Electronic circuitry. A fast-slow system was used with an 80-nanosecond resolving time. The electron pulses were selected for pulse height and the coincident α-particle pulses were recorded by the multichannel analyzer. The gating supply synchronized the delayed counting cycle.

circuit consisted of linear amplifiers, scalers, the single-channel discriminator which selected the energy of the coincident beta spectrum, and the 100-channel analyzer which recorded the alpha spectrum. A coincidence was registered in the 100-channel analyzer when four conditions were satisfied within its 1-μsec resolving time: (1) the gating switch was open for the 0.4-sec counting period, (2) the fast coincidence mixer produced an output pulse, (3) the beta-single channel discriminator produced an output pulse, and (4) the alpha amplifier produced an output pulse.

III. EXPERIMENTAL PROCEDURE

For the purpose of analysis, the data were collected into groups of about 1000 B^8 or 10 000 Li^8 coincidences at each angle, typically an entire day's results. The position of the beta detector was changed after each run of about 15 min in order to minimize the effects of slow variations in gain or target conditions. Before, after, and several times during a set of coincidence runs, spectra of the non-coincident alpha particles and electrons were also recorded. An alpha-particle energy spectrum is shown in Fig. 5 for the Li^8 beta decay. The gain was adjusted to give a similar spectrum for each group of runs. The points marked "$\alpha-\alpha$ coincidence gate" in Fig. 5 represent the same spectrum but with the added requirement of an output pulse from the fast coincidence mixer when the same alpha-particle pulses are fed into both inputs. With an 80-nsec resolving time the coincidence mixer was not very sensitive to the low frequency noise from the surface barrier detectors, but the coincidence mixer was evidently sensitive to alpha

[21] M. E. Nordberg, Bull. Am. Phys. Soc. 4, 457 (1959); for details of detector construction see G. Dearnaley and A. B. Whitehead, Atomic Energy Research Establishment Report No. R3662 (unpublished); and Nuclear Instr. and Methods (to be published).

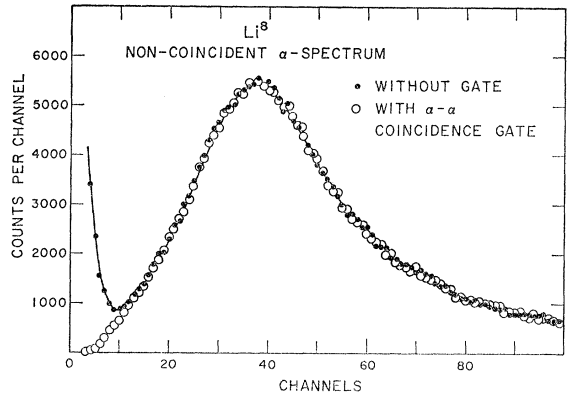

FIG. 5. The α-particle pulse height spectrum from the gold-silicon detector following the Li^8 beta decay. The points marked "$\alpha-\alpha$ coincidence gate" tested the operation of the fast coincidence mixer. The spectrum extends nearly to zero pulse height because of the alpha-particle energy loss in the target and the limited resolution of the detector.

particles of pulse height at least as low as channel 10. The alpha-particle spectra for the B^8 beta decay were similar but slightly broader and with somewhat more noise because of the lower alpha-particle yield.

The electron energy spectrum for the Li^8 beta decay is shown in Fig. 6. Background counts were subtracted by taking a run of equal time with the target reversed. The B^8 beta spectrum exhibited much more low-energy background but otherwise was similar. The beta spectrum with the requirement of an output pulse from the single channel discriminator was also recorded and corresponds to the shaded portion of Fig. 6 for an average beta energy of about 11 Mev. The dashed curve of Fig. 6 represents the Li^8 beta spectrum obtained by Hornyak and Lauritsen[22] with a magnetic spectrometer. It is plotted to have the same area as the experimental curve and the upper half-maximum points

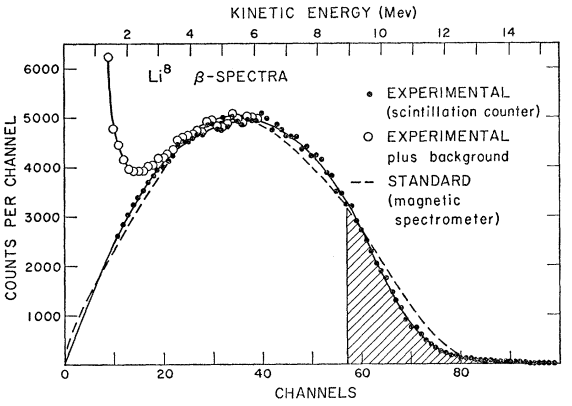

FIG. 6. Electron pulse height spectrum of the Li^8 beta decay. The experiment measured the number of alpha particles in coincidence with the beta pulses in the shaded region of the spectrum. The energy was determined by comparison with the spectrum from a magnetic spectrometer.

[22] W. F. Hornyak and T. Lauritsen, Phys. Rev. **77**, 160 (1950).

have the same abscissa. From the work with the magnetic spectrometer, the kinetic energy of the point of half-maximum is known to be 9.5 Mev. This point was used to calibrate the scale of the observed spectrum and thus to determine the average energy of the shaded portion. For the B^8 beta spectrum the energy of the point of half maximum was taken as 9.5 Mev times the ratio of end point energies for beta decay to an assumed sharp level at 2.90 Mev. During coincidence runs, the total number of counts in the shaded portion was recorded and the coincidences were normalized by dividing by this number.

The alpha-spectra of a normalized set of coincidence runs are shown in Figs. 7 and 8 for the Li^8 and B^8 beta decays with average electron energies of about 11 Mev. All coincidences of pulse height over channel 100 were automatically recorded by the 100-channel analyzer and

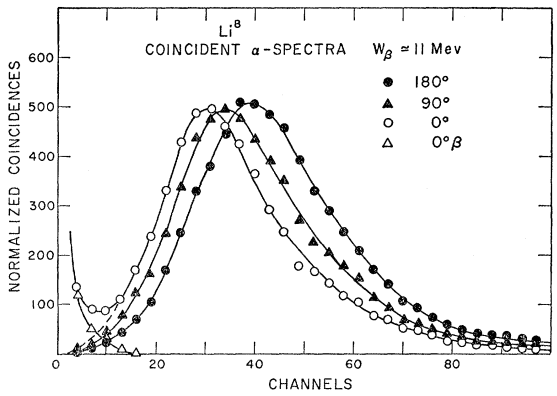

FIG. 7. The alpha-particle pulse height spectra in coincidence with electrons from the Li^8 beta decay at various angles. A prominent feature of the curves is the energy shift with angle which is the result of the Be^{8*} recoil from the beta decay. This experiment measured the total areas of the curves to determine the coefficients of the angular distribution, $W(\theta_{\beta\alpha})=1+A\cos\theta_{\beta\alpha}+B\cos^2\theta_{\beta\alpha}$. The points marked "0°$\beta$" were the response of the gold-silicon detector to the electrons.

were used in determining the total areas under the curves. At low pulse heights, the 0° spectrum was complicated by the fact that electrons passing through the alpha detector into the beta detector, produced small pulses in the alpha detector which were in coincidence with the pulses of the beta detector. If the target was turned so that all of the alpha particles were stopped in the target backing, the electrons, which easily penetrate the backing, produced the small spectrum labeled "0°β" in Figs. 7 and 8. These spurious coincidences were subtracted to obtain the true 0° spectra.

Because the B^8 spectra are broader, from the greater energy loss of the alpha particles in the target, the low-energy region contains more coincidences and therefore the extrapolation to zero pulse size represents a somewhat larger uncertainty than in the Li^8 spectra. However, a considerable improvement in the measured alpha spectra was obtained by placing the target so

that the angle of incidence of the beam was 75°, and by shielding the alpha detector while the beam was on the target. The contrast between the 90° coincident alpha spectra from our preliminary experiment[16] with a 60°-angle of incidence and no target shield, and the present experiment is illustrated in Fig. 9.

The energy available in the transition from Li^8 or B^8 to two alpha particles, is shared among the β ray, neutrino, and the two alpha particles. With lower energy electrons, correspondingly higher energy alpha particles may be in coincidence. This feature of the data is shown in Fig. 10 for the Li^8 case.

Corrections for the number of random fast coincidences were determined by making some runs with added delay in the beta system. The number of random coincidences was significant only for the Li^8 decay with its higher counting rate, and even then amounted to only 2–3% of the number of real coincidences.

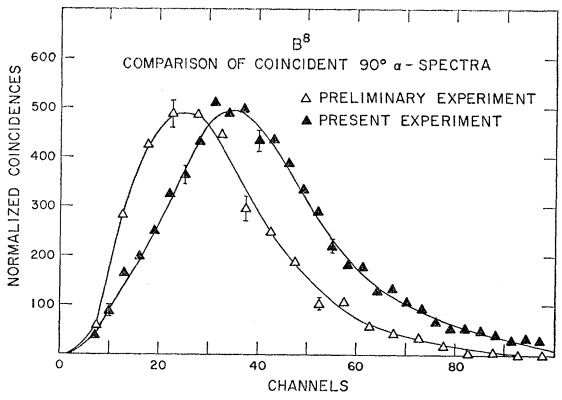

FIG. 9. Comparison of the 90° coincident alpha spectra from the B^8 beta decay in the preliminary measurement and the present experiment. The present experiment has less possibility of systematic error from inaccurately determining the number of coincidences at low pulse height.

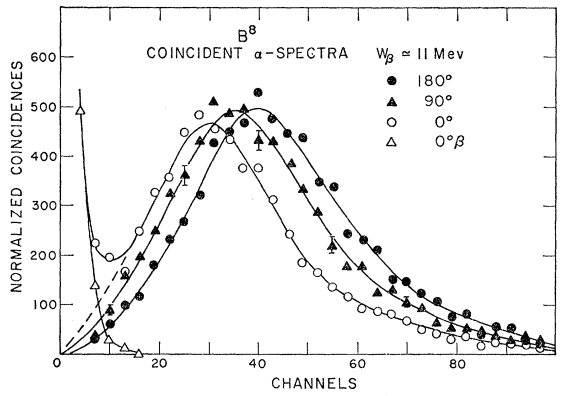

FIG. 8. The alpha-particle pulse height spectra in coincidence with positrons from the B^8 beta decay at various angles. Statistics are poorer in this case than in Fig. 7 because of the lower counting rates and the curves are broader because of increased α-energy loss in the target backing.

IV. RESULTS AND DISCUSSION

A. Analysis of Results

For each group of runs the numbers of coincidences, $n(0°)$, $n(90°)$, and $n(180°)$, were obtained by summing the coincident alpha-spectra, normalized as explained in Sec. III. These numbers determine the coefficients, A and B, from Eqs. (8) and (9). The coefficients were both divided by W_β in order to average together several groups of data taken with slightly different beta energies, and for comparison with theory. In the averaging procedure the coefficients were weighted with the inverse square of the statistical error which, for a single group, was much larger than the estimated systematic error. The overall averages of the coefficients are tabulated in Table I.

Histograms of the results of all the groups of runs are shown in Fig. 11. To check the internal consistency of the data, normal distribution curves have been drawn, centered at the weighted means of the $W_\beta \simeq 11$-Mev data, and with widths equal to $\sqrt{N}$ times the statistical standard deviations of the weighted means, where N is the number of groups of data included in each of the histograms. The fact that in no case is the histogram much broader than the statistical expectation is an indication that systematic errors are either constant over all groups or small.

The value of the coefficient, B, for the Li^8 decay has previously been measured with less accuracy by Bunbury[23]; Hanna, LaVier, and Class[24]; and more recently, with better precision, by Krebs, Rieseberg, and Soergel.[25] Their results are listed in Table II, together with the results of the present experiment. The B^8 beta-alpha correlation has not been measured previously.

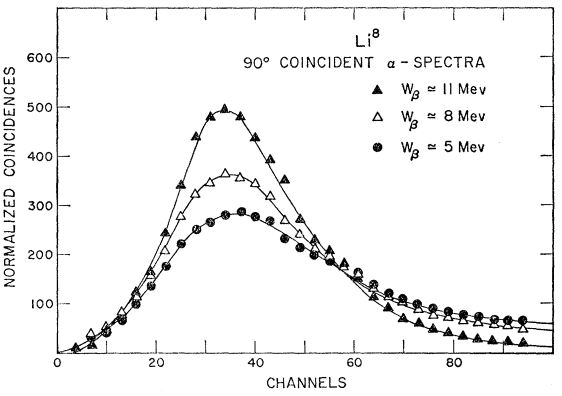

FIG. 10. Comparison of the 90° coincident alpha spectra from the Li^8 beta decay at three electron energies. The shapes of the curves are the effect of the conservation of energy and the sharing of the 16-Mev Q value among the electron, neutrino, and two alpha particles.

[23] D. St.P. Bunbury, Phys. Rev. **90**, 1121 (1953).
[24] S. S. Hanna, E. C. LaVier, and C. M. Class, Phys. Rev. **95**, 110 (1954).
[25] K. Krebs, H. Rieseberg, and V. Soergel, Z. Physik **159**, 232 (1960).

TABLE I. Experimental values of the coefficients A and B, with statistical and estimated systematic errors (in units of 10^{-4}).

β decay	W_β (Mev)	Coefficient	Result	Statistical error	Estimated systematic errors				Combined error
					W_β	α spectrum	Counting rate	Symmetry	
Li^8	5	A/W_β	−73	6	8	2	1	4	11
		B/W_β	23	8	4	2	1	4	10
Li^8	8	A/W_β	−72	6	8	3	1	3	11
		B/W_β	33	8	4	3	1	3	10
Li^8	11	A/W_β	−87	2	4	4	1	2	7
		B/W_β	31.6	2.8	2	4	1	2	6
B^8	11	A/W_β	−87	5	5	4	···	4	9
		B/W_β	−38.6	7.3	2	4	···	4	10
Li^8-B^8	11	δ/W_β [a]	70	8	4	3	1	6	12

[a] $\delta = B(Li^8) - B(B^8)$.

B. Estimates of Systematic Errors

Aside from statistical errors, which were computed in a straight-forward manner, several possible sources of systematic error have been considered and are discussed below. Estimates of these errors are listed in Table I. The over-all errors listed in Table I are the root mean square sums of the statistical and estimated systematic errors.

1. Beta Spectrum

Since the coefficients are divided by W_β for comparison with theory, a small percentage error in the determination of W_β contributes an equal percentage error to the quantities, A, B, and δ. Such an error does not tend to cancel in taking the Li^8-B^8 difference.

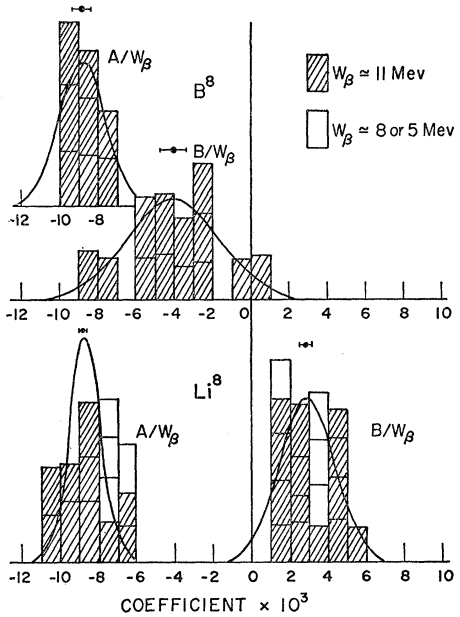

FIG. 11. Histogram of results. The results of 13 runs for the B^8 case and 18 runs for the Li^8 case are shown. The weighted mean values of the coefficients and their statistical errors are indicated above each of the histograms. The normal curves give the expected distributions of measurements at $W_\beta = 11$ Mev on the basis of statistical errors only.

As discussed above, the average beta energy was determined by comparing the average pulse size selected by the beta discriminator with the pulse size corresponding to the upper half-maximum point of the beta spectrum. From the work with a magnetic spectrometer the true beta-spectrum is known with a degree of accuracy more than adequate for the purposes of this experiment. An approximate graphical method of smearing the true spectrum with the counter resolution produced a curve which closely followed the observed spectrum and, in addition, indicated that the upper half-maximum point was almost unaltered by the smearing process. Approximate computations also showed that the average energy of the selected pulses was changed by no more than 2% by the asymmetrical resolution of the beta counter. It is, therefore, estimated that the systematic error in W_β is less than 5% for the high beta-energy groups of data. This leads to an error in δ of less than half of the statistical error. For the 5- and 8-Mev groups of data, the limit of systematic error in W_β may reasonably be set at 10%, which is relatively less important since the statistical accuracy of the lower beta-energy data is poorer.

2. Alpha Spectrum

The problem of integrating over the low-energy region of the coincident alpha spectrum is aggravated by three factors: the breadth of the 2.90-Mev level, the change in the coincident alpha spectra with angle, and the loss of energy in the target. The last factor was different in the Li^8 and B^8 decays because of the difference in incident beam energies and masses. Taken together, the three effects suggest the possibility of errors which would be different for the 0°, 90°, and 180° spectra, and which would not have cancelled in the Li^8-B^8 difference. Such errors would have occurred if the coincidence mixer did not function properly on small pulses. In addition to the alpha-alpha curve of

Fig. 5, several other checks have been made to ensure the proper operation of the coincidence mixer. A pulser in place of the alpha detector registered with 100% efficiency down to channel 8 and counted below that with somewhat reduced efficiency. With the slow amplifier at a fixed gain, the number of coincidences in channel 10 remained constant until the signal into the coincidence mixer was reduced by about a factor of 2 below normal operating conditions by decreasing the fast amplifier gain. The fact that two quite different coincidence mixers were used in the course of the experiment with no apparent difference in results is also an indication of the reliability of the coincidence mixer.

As a consistency check, the coincidences taken at 0° were neglected and the values of B were calculated for the 11-Mev data, from Eq. (10) with the assumption, $A=(-0.0087)W_\beta$. As a result, B_{Li^8} decreased by $(0.0004)W_\beta$ and B_{B^8} decreased by $(0.0002)W_\beta$, giving a net decrease in δ of $(0.0002)W_\beta$. When the values of B were calculated from the 0° and 90° data alone, again assuming $A=(-0.0087)W_\beta$, B_{Li^8} increased by $(0.0002)W_\beta$, while B_{B^8} increased by $(0.0001)W_\beta$. This yields an increase in the value of δ of $(0.0001)W_\beta$. We have taken these changes in B_{Li^8}, B_{B^8}, and δ as an indication of the magnitude of the systematic errors in these quantities, determined from the data including all three angles, due to the small pulse height region of the alpha spectra.

3. Counting Rate Effects

Effects associated with the counting rate were small for the Li^8 decay and negligible for the B^8 decay for which the counting rate was at least a factor of ten lower. The major correction, which amounted to only about 2–3% of the real coincidences, was that for random coincidences in the fast coincidence mixer. These were experimentally measured and subtracted. Random coincidences in the slow coincidence mixer were not measured but were calculated to be at least five times smaller and, in any case, would have been important only if the counting rate had been a systematic function of the position of the beta detector. Errors due to dead time losses in the beta discriminator were eliminated by normalizing the coincident counts to the selected noncoincident beta counts.

4. Geometrical Symmetry

Although small variations in solid angles of the beta detector would not have been serious, since the coincidences counts were normalized to the selected beta counts, axial symmetry was preserved as much as possible; the Lucite target chamber walls were turned to uniform thickness, and dummy alpha counters were placed at symmetrical positions in the chamber. Tests of symmetry with radioactive sources fixed to the target rod, as well as with fixed quantities of integrated beam on the lithium target, showed no systematic asymmetry in counting rate for either beta or alpha detector.

To keep the solid angle of the alpha counter constant, the lithium was evaporated in a thin vertical strip on the target, and the target and alpha counters were mounted from the top of the target chamber. The constancy of the solid angle of the alpha counter was checked by taking the ratio of noncoincident counts in the alpha counter to those in the monitor counter, as the angular position of the beta counter was changed. This ratio varied less than 0.2% on the average, which is adequate for the present experiment.

The background counting rate in the beta counter, which came largely from neutrons and γ rays produced by the chopped beam, would not be expected to be the same in the various positions of the beta counter. Since the counts selected by the single-channel analyzer on the beta counter were used for normalization, it was necessary to select β rays of sufficiently high energy that the background counting rate was negligible for both Li^8 and B^8 runs. This background prevented selection of beta energies lower than $\sim$10 Mev for the B^8 case, while runs could still be made at $W_\beta \simeq 5$ and $\simeq 8$ Mev with Li^8 because of its large production cross section.

TABLE II. Measurements of the coefficient B in the distribution $1+A\cos\theta_{\beta\alpha}+B\cos^2\theta_{\beta\alpha}$.

β-decay	B/W_β	Statistical error	W_β(Mev)	Reference
Li^8	0.004	±0.020	9.8	Bunbury[a]
Li^8	0.016	±0.012	7.5	Bunbury[a]
Li^8	0.002	±0.006	6	Hanna *et al.*[b,c]
Li^8	0.0057	$+0.0029$ -0.0019	7.0	Krebs *et al.*[d]
Li^8	0.0054	$+0.0074$ -0.0066	3.5	Krebs *et al.*[d]
Li^8	0.0032	±0.0003	10.8	Present experiment
Li^8	0.0033	±0.0008	8.1	Present experiment
Li^8	0.0023	±0.0008	5.6	Present experiment
B^8	-0.0039	±0.0007	11.1	Present experiment

[a] See reference 23. In this reference no mention was made of the $\cos\theta_{\beta\alpha}$ term and measurements were carried out only between 90° and 180°. The values quoted are, therefore, probably the quantity, $(B-A)/W_\beta$, of this experiment.
[b] See reference 24.
[c] The average value of B over most of the beta spectrum is used together with an approximate average energy.
[d] See reference 25.

V. CONCLUSIONS

From the measured values for β rays of $\sim$11 Mev,

$$B_{\mathrm{Li}^8}=(0.00316\pm0.00060)W_\beta$$

and

$$B_{\mathrm{B}^8}=(-0.00386\pm0.00100)W_\beta,$$

we obtain $\delta=(0.0070\pm0.0012)W_\beta$. This value may be compared with Weidenmüller's theoretical predictions,[16]

$$\text{C.V.C. theory:}\quad 0.005\,W_\beta<\delta<0.009\,W_\beta,$$

$$\text{Fermi theory:}\quad 0.001\,W_\beta<\delta<0.004\,W_\beta.$$

The measured value lies within the range of the theoretical values of of δ for the conserved vector current theory and disagrees with the prediction of the older theory, which includes no pion corrections. It must be recalled, however, that the theoretical predictions depend on calculated values of the $M1$ and $E2$ γ-ray matrix elements for Be^8. Although there is no reason to doubt that ample allowance has been made for uncertainties in the theoretical calculations, it is clearly important to measure $\Gamma_\gamma(M1)$ and $\Gamma_\gamma(E2)$ for the $J=2^+$, $T=1$ level of Be^8 which is the analog of the Li^8 and B^8 ground states. If we assume the validity of the conserved vector current theory the present experiment indicates that $\Gamma_\gamma(M1)=(1.9\pm0.6)$ ev.

Although the principal result of the present experiment is the measured value of δ, there is also some statistically weak evidence in the measured values of the A and B coefficients for the presence of axial vector-axial vector interference terms which were not included in deriving Eq. (7). The experimentally determined values, $A_{Li^8}=(-0.0087\pm0.0007)W_\beta$ and $A_{B^8}=(-0.0087\pm0.0009)W_\beta$, are both lower than the value derived from the first order term of Eq. (7),

$$\frac{-W_\beta}{c}\langle 1/p_\alpha\rangle \simeq (-0.0093)W_\beta.$$

In addition, the second-order term in the B coefficient,

$$\frac{5W_\beta^2}{8c^2}\langle 1/p_\alpha\rangle^2,$$

predicts that $|B_{Li^8}|-|B_{B^8}|$ should be $(+0.0006)W_\beta$, while the experiment gives the value $(-0.0007\pm0.0012)W_\beta$.

ACKNOWLEDGMENTS

The authors would like to thank Dr. H. A. Weidenmüller for many fruitful discussions, and Professors William A. Fowler and T. Lauritsen for valuable comments and criticism.

APPENDIX A

In the Be^{8*} rest system, the angular correlation function of the electron, neutrino, and one of the oppositely directed alpha particles is the following[26]:

$$W(ea,en,na)=1-\tfrac{1}{3}aW_\beta-(1-\tfrac{1}{3}aW_\beta)\cos ea\cos na - aW_\beta\cos en+aW_\beta\cos^2 ea,$$

where ea, en, and na are the angles between the electron and alpha particle, etc.; the quantity, a, is the interference term from the $M1$ type matrix element only. The approximation, $p_\beta c=W_\beta$, is assumed. The transformation to the laboratory system is expressed in the general identity:

$$W(en,ea,na)d\Omega_e d\Omega_n d\Omega_a = W[en(\beta\nu,\beta\alpha,\nu\alpha),\ ea(\beta\nu,\beta\alpha,\nu\alpha),\ na(\beta\nu,\beta\alpha,\nu\alpha)] \times\frac{d\Omega_e d\Omega_n d\Omega_a}{d\Omega_\beta d\Omega_\nu d\Omega_\alpha}d\Omega_\beta d\Omega_\nu d\Omega_\alpha,$$

where $\beta\nu$, $\beta\alpha$, and $\nu\alpha$ are the laboratory angles between particles. Since the recoil velocity of the Be^{8*} nucleus is much less than the velocity of the neutrino or electron, $d\Omega_e/d\Omega_\beta\simeq1$, $d\Omega_n/d\Omega_\nu\simeq1$, and $en\simeq\beta\nu$ to very good approximations. The remaining ratio, $d\Omega_a/d\Omega_\alpha$, is expressed in terms of the Jacobian which can be calculated from the equations for the conservation of momentum. The conservation of energy can be neglected because the recoil energy of the Be^{8*} nucleus is at most 15 kev of the total 16-Mev Q value. Integrating the resultant correlation function over the unobserved neutrino direction gives the distribution, $W(\theta_{\beta\alpha})$. This is further approximated by averaging the reciprocal of the α-particle momentum in terms of the 90° coincident spectrum, which adds part of the small $\cos^2\theta_{\beta\alpha}$ term, and by combining a small $\cos^3\theta_{\beta\alpha}$ term with the $\cos\theta_{\beta\alpha}$ term. The result is given by Eq. (7).

[26] H. A. Weidenmüller (private communication).